



저작자표시-비영리-변경금지 2.0 대한민국

이용자는 아래의 조건을 따르는 경우에 한하여 자유롭게

- 이 저작물을 복제, 배포, 전송, 전시, 공연 및 방송할 수 있습니다.

다음과 같은 조건을 따라야 합니다:



저작자표시. 귀하는 원저작자를 표시하여야 합니다.



비영리. 귀하는 이 저작물을 영리 목적으로 이용할 수 없습니다.



변경금지. 귀하는 이 저작물을 개작, 변형 또는 가공할 수 없습니다.

- 귀하는, 이 저작물의 재이용이나 배포의 경우, 이 저작물에 적용된 이용허락조건을 명확하게 나타내어야 합니다.
- 저작권자로부터 별도의 허가를 받으면 이러한 조건들은 적용되지 않습니다.

저작권법에 따른 이용자의 권리는 위의 내용에 의하여 영향을 받지 않습니다.

이것은 [이용허락규약\(Legal Code\)](#)을 이해하기 쉽게 요약한 것입니다.

[Disclaimer](#)

Thesis for the Degree of Master of Engineering

Study on Crosslinkable Poly(vinylidene
difluoride) (PVDF) Battery Binders toward
Stable Silicon Anode Performance

by

Young Je Kwon

Department of Industrial chemistry

The Graduate School

Pukyong National University

February 2022

Study on Crosslinkable Poly(vinylidene difluoride)
(PVDF) Battery Binders toward Stable Silicon
Anode Performance

(안정적인 실리콘 음극성능을 위한
가교가능한 PVDF 배터리 바인더 연구)

Advisor: Prof. Kie yong Cho, Prof. Min yong shon,

By
Young Je Kwon

A thesis submitted in partial fulfillment of the requirements
for the degree of

Master of Engineering

in Department of Industrial Chemistry, The Graduate School,
Pukyong National University

February 2022

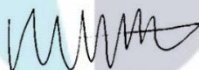
Study on Crosslinkable Poly(vinylidene difluoride) (PVDF) Battery Binders
toward Stable Silicon Anode Performance

A dissertation
by
Young Je Kwon

Approved by :



(Kie Yong Cho)



(Min-yong Shon)



(Sujong Chae)

February 25, 2022

Contents

Contents	i
List of Figures	iii
Abstract	vi

1. Introduction.....1

1-1. The Background of Si anode.....	1
1-2. The Background of Binder.....	5
1-3. Efficient Binders for Silicon-based Lithium-ion Battery,,.....	8
1-4. PVDF Binder	10
1-5. PVDF Modification.....	11

2. Experimental14

2-1. Materials	14
2-2 Synthesis of double bond-contained PVDF-CTFE (PVTD).....	15

2-3 Prepare of Electrode.....	16
2-4 Characterization	17
2-5 Electrochemical Characterization.....	19

3. Results and discussion.....20

3-1 Electrochemical characterization.....	20
3-2 Strategy of Cross-linked PVDF-Based Polymers (PVTDX).....	22
3-3 Processibility of PVTDX Binder.....	26
3-4 Cross-link of PVTDX Polymer Binder.....	30
3-5 Electrochemical Performance of PVTDX Binder.....	38
3-6 SEI Contribution of PVTDX Binder.....	45
3-7 Interfacial Adhesion with Electrode	47

4. Conclusions.....49

References51

List of Figures

Figure 1. (a) Gravimetric Capacity and (b) Volumetric Capacity of each anode material.....	2
Figure 2. Illustration of Problems in the electrode of a silicon anode.....	4
Figure 3. The role of the binder in the electrode (a) Bonding action, (b) Volume Change Alleviation, (c) Dispersing Function, (d) conductivity.....	8
Figure 4. Modification methods of PVDF-based polymers.....	13
Figure 5. Schematic mechanisms for Si anode with (a) conventional leaner PVDF binders (PVDF and PVDF-CTFE) and (b) cross-linked PVDF binder (PVTDX).....	21
Figure 6. Mechanism of PVTD (Using Dehydrochlorination of PVDF-CTFE Dehydrochlorination.....	24
Figure 7. (a) ^1H NMR and (b) ^{19}F NMR of PVDF-CTFE and PVTD..	24
Figure 8. FT-IR spectra of PVDF-CTFE and PVTD.....	25
Figure 9. . (a) Chemical structure of PVDF and PVTD with their crystalline phases. (b) FT-IR Spectra.....	28
Figure 10. Complex viscosity curves of PVDF,PVDF-CTFE and PVTD.....	29

Figure 11. DSC data of PVDF,PVDF-CTFE and PVTD.....	29
Figure 12. The schematic illustration for before and after a cross- linking process of PVTD.....	31
Figure. 13. 1 st run DSC heating curves for PVTD and PVTDX.....	32
Figure. 14. FT-IR spectra for PVTD and PVTDX.....	32
Figure 15. (a) Photographs for the solvent resistance test in DMF before and after 24 h later. (b) GPC Data of DMF solution at 24hr after.....	34
Figure. 16. S-S curves of PVTD and PVTDX.....	36
Figure 17. TGA (inset: 5% degradation point)of PVTD and PVTDX.....	37
Figure 18. Cyclic voltammetry curves of silicon anode with (a) PVDF and (b) PVTDX binder.....	39
Figure. 19. Charge/discharge profiles at 10 th , 30 th , 50 th , 100 th of silicon anode with (a)PVDF and (b)PVTDX binder.....	40
Figure. 20. (a) Rate capability at various current densities. (b) Cycling performance at 1 A/g.....	42
Figure. 21. S-S curves of PVDF, PVDF-CTFE and PVTDX.....	44
Figure. 22. Before and after electrolyte stability tests at RT (1 M LiPF ₆ in EC/DEC (50:50 v/v): OM images images for PVDF and PVTDX thin films (inset: their photographs).....	44

Figure. 23. Cross-section SEM images of silicon anode before and after cycling with (a) PVDF, and PVTDX binders. XPS spectra of (b) C 1s, (c) F 1s and (d) Li 1s peaks on the surface of silicon anode with PVDF and PVTDX binders after 100 cycles.....46

Figure 24. (a) Adhesion and Cohesion illustrate. Adhesive properties of the silicon anode using different binders : (b) Force-displacement curves and (h) peel strength.....48



Study on Crosslinkable Poly(vinylidene difluoride) (PVDF) Battery Binders toward Stable Silicon Anode Performance

Young Je Kwon

in Department of Industrial Chemistry, The Graduate School,
Pukyong National University

Abstract

In recent years, the electric vehicle market is increasing the demand for high energy density storage devices such as lithium ion batteries applied in portable electronic devices, electric vehicles (EVs) and intermediate storage of renewable energy.

Lithium battery applications demand higher performance for cycle life, capacity retention and reliability. Si is an ideal lithium-ion battery (LIB) anode material due to its excellent capacity and suitable voltage. However, large volume changes (~420%) of Si anode during the charge/discharge cycle lead to the collapse of the anode, resulting in a very unstable cycle.

Polymer binders are one of the methods of efficient suppressing large volume expansion of Si anode. However, the conventional electrode binder, PVDF (Poly vinylidene Fluoride), lacks the ability to suppress Si deformation.

To overcome the deficiency characteristics of PVDF binder, a 3D Cross-linked network was formed through chemical modification of the polymer. The 3D network polymer binder exhibits high battery stability compared to conventional PVDF due to its high mechanical strength that limits the volume expansion of Si particles. PVDF-based binders provide a new avenue for the development of Si anodes for high-energy-density lithium-ion batteries

안정적인 실리콘 음극성능을 위한 가교가능한 PVDF 배터리 바인더 연구

권영제

부경대학교 대학원 공업화학과

요 약

최근 전기 자동차 시장은 휴대용 전자 장치, 전기 자동차(EV) 및 재생 가능 에너지의 중간 저장 장치에 적용되는 리튬 이온 배터리와 같은 고에너지 밀도 저장 장치에 대한 수요가 증가하고 있다. 리튬 배터리 애플리케이션은 사이클 수명, 용량 유지 및 안정성에 대해 더 높은 성능을 요구된다. Si 음극재는 뛰어난 용량과 적절한 작동 전압으로 인해 이상적인 리튬 이온 배터리(LIB) 음극재이다. 그러나 충 방전 사이클 중 매우 큰 부피 변화(~420%)는 음극의 붕괴를 초래하며, 이는 매우 불안정한 사이클을 초래하여 전극의 안정성을 낮춘다.

고분자 바인더는 고성능 Si 의 큰 부피 팽창을 제한하기 위한 음극의 효율적인 방법 중 하나입니다. 그러나 기존의 전극 바인더인 PVDF(Poly vinylidene Fluoride)는 Si 변형을 억제하는 성능이 부족하다.

PVDF 바인더의 결핍 특성을 극복하기 위해 폴리머의 화학적 개질을 통해 3차원 가교 네트워크를 형성했다. 3차원 네트워크 폴리머 바인더는 Si 입자의 부피 팽창을 제한하는 높은 기계적 강도로 인해 기존 PVDF에 비해 높은 배터리 안정성을 나타낸다. PVDF 기반 3 차원 구조의 바인더는 고에너지 밀도 리튬 이온 배터리용 Si 양극 개발에 있어서 새로운 방향성을 제시한다.

1. Introduction

1-1. The Background of Si anode

In the last years, Li-ion batteries (LIBs) is one of the most efficient rechargeable batteries. As energy storage at the KWh level is required, the storage capacity needs to be greatly improved. However, the graphite anode used for commercial use has a low theoretical capacity (372 mAh g⁻¹). Cathode materials capable of storing a higher level of energy are required. An Dey et al. demonstrated that Li metal can electrochemically alloy with other metals (Sn, Pb, Al, Au, Pt, Zn, Ag, Mg, and Cd) at room temperature.¹ However, metal anode materials use is limited for toxic property. Among the various Li alloy elements, Si not only exhibits the highest theoretical capacity (4200 mAh g⁻¹) but also is the second most abundant element on the surface of the earth. Si is inexpensive, low toxicity and harmless to the environment. (Table 1)(figure 1) Accordingly, Si has been considered as one of the most attractive anode materials for LIBs.²

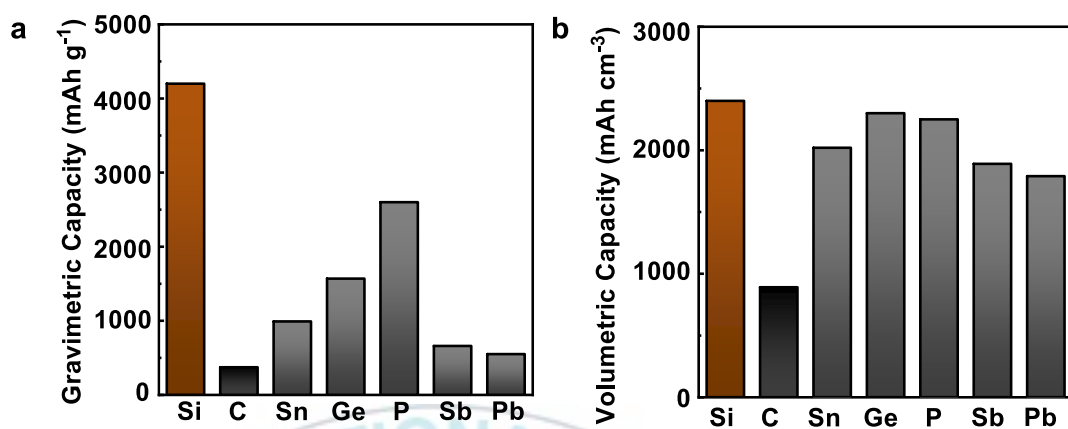


Figure 1. (a) Gravimetric Capacity and (b) Volumetric Capacity of each anode material.

Table 1. Property of Li alloy elements.

Element	Gravimetric capacity (mAh g ⁻¹)	Volumetric capacity (mAh cm ⁻¹)	Cost	Toxicity	Safety
Si	4,200	2,400	Low	No	High
C	372	890	Low	No	Low
Ge	1,568	2,300	High	High	High
Sn	990	2,020	Low	No	High
P	2,600	2,250	Low	High	Low
Sb	660	1,890	Low	High	Low
Pb	549	1,790	Low	High	Low

However, Si suffers from rapid capacity fading, which greatly hinders its application as a commercial anode material. The silicon anode changes to the form of Li_xSi_y in alloy with Li, resulting in volume expansion of up to 420% (Figure. 2). In addition, there are problems such as pulverization of particles and excessive growth of the SEI layer according to a large volume change, causing rapid capacity fading³, shortening cycle life⁴, and isolation of the anode from the electrode, separated from the void and the electrode⁵. Therefore, it is necessary to suppress this volume expansion for commercial use of the Si anode. Mazouzi D et al showed that high efficiency can be secured depending on the binder and formulation in the maintenance of the silicon electrode⁶. Thus, binders have become a non-ignorable part although merely occupy a small mass content.

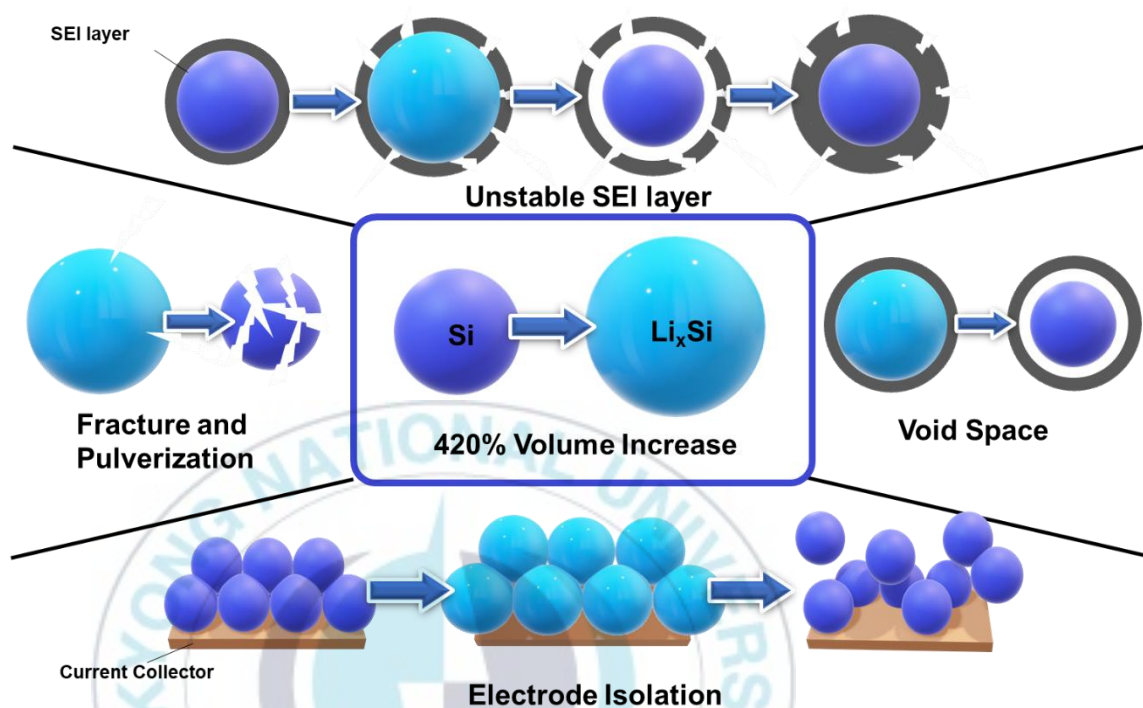


Figure 2. Illustration of Problems in the electrode of a silicon anode.

1-2. The Background of Binder

As such, silicon anodes are being promoted as one of the promising candidates for next-generation high-capacity electrodes because of their very large theoretical capacities. However, it is necessary to suppress large volume changes. Accordingly, the role of the binder has become important. The binder initially accounts for less than 10 wt% of the electrode but is one of the important factors throughout the cell. Basically, the binder is used to bond the active material and the conductive agent to the current collector. However, with the advent of silicon-based anode materials, the function of the binder was to secure mechanical stability and to manipulate the characteristics of the battery.

First, the basic role of the binder is to allow the active material and the conductor to be attached to the current collector Fig. 3a. three different binder polymers layers appear when binder contact with active material particles or conductive agent particles: bonded layer, fixed layer, and excessive polymer layer. Formation of a polymer layer bonded by mechanical interlocking effect. Excessive polymer layer surrounding the fixed layer is constructed by free polymers and

combined with the current collector. Besides the above mechanism, another model including adsorption (thermodynamic) or wetting theory, acid-based theory, diffusion theory, and weak boundary layers theory have been proposed. It should be noted that a single model or theory cannot fully explain complicated binding mechanism of binders in LIBs.⁷

Second, the suppression of the enormous volume change of the Si-based electrode (Fig. 3b). The cycling stability of Si-based electrodes is poor due to the huge volume change. At this time, the polymer binder can control the mechanical stress induced by the Si volume change. When external mechanical force due to expansion transmitted to polymer layer is less than adhesion force, the binder system can alleviate the volume change of Si anode by maintaining polymer layer.⁸

The third is the Dispersing function (Fig. 3c). The main challenge in preparing the slurry is to prevent aggregation induced by the interaction of the materials. High dispersibility through uniform distribution can not only increase adhesive strength, but also efficiently support the formation of the SEI layer. Carbon black, one of the frequently used

conductive agents, has small particles and a large specific surface area, so aggregation occurs easily⁹. The binder serves to separate and disperse the materials of the electrode body and the conductor and promotes uniform distribution of the mixture. In particular, when there is a polar group, it has high dispersibility to wrap the outside through interaction with Si, and interaction with carbon when there is a π - π function^{10,11}. In this way, aggregation can be prevented through a binder.

Finally, the conductivity of electrons and ions(Fig 3d). In the case of conventional polymer binders, this part is electronically insulated, increasing the resistance of the entire system, and lowering the ionic conductivity. However, by attaching a polar group to improve ionic conductivity and developing a conductive binder, conductivity can be significantly improved than before. Comprehensive understanding of the function of the above binder is very important for the development of a functional binder that meets the requirements of anodes, especially Si anodes. By improving the above performances, the problem of the Si anode can be improved, and the performance of the LIB can be further improved.¹²

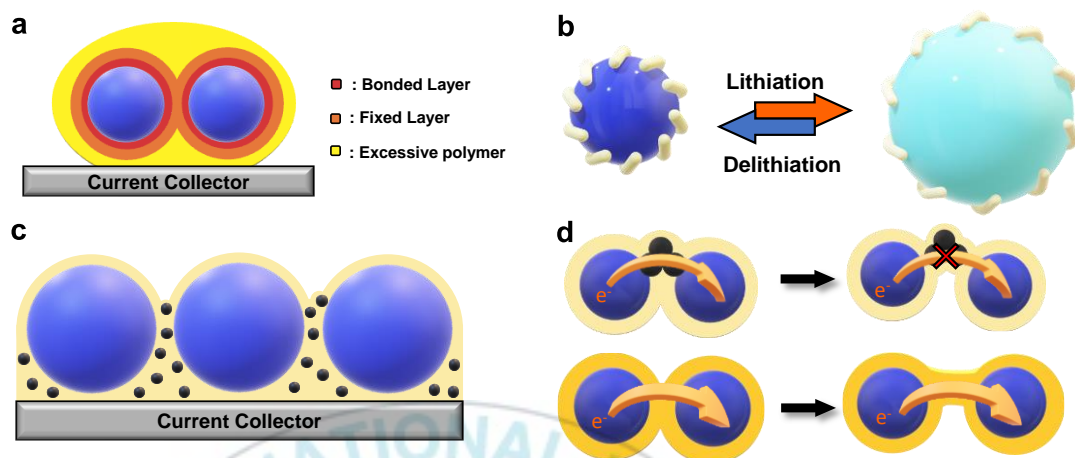


Figure 3 The role of the binder in the electrode (a) Bonding action, (b) Volume Change Alleviation, (c) Dispersing Function, (d) conductivity

1-3. Efficient binders for silicon-based lithium-ion battery

Based on the conditions for an efficient polymer for the silicon anode, various strategies were used to realize a silicon electrode with high capacity and long cycle life in Songdo, and various polymer binders were also tried. However, the existing PVDF binder is dependent on the van der Waals force when connecting the components in the electrode, which is too weak to be used for the Si electrode with large volume

change. Accordingly, PVDF was replaced with CMC or PAA to achieve improved performance based on improved adhesion through polar polymers.¹³ However, the polymer binder weakened or even lost due to the expansion of the silicon anode. Accordingly, in order to secure high performance of the electrode, it is necessary to prevent dissociation of the polymer due to the volume expansion of the polymer binder. Accordingly, polymers of various structures have been developed. The crosslinked polymers offer a great opportunity and flexibility to the binder design. Compared to polymers with a linear structure, polymers with interconnected networks have significantly improved mechanical strength. In addition, the Si particles can be tightly anchored, effectively improving adhesion. In addition, crosslinking through different heterogeneous polymers, the combination of hard and soft polymer chains can provide great flexibility and strong mechanical strength to accommodate volume expansion. Therefore, in this study, based on PVDF, which is a linear polymer with clear limitations, a cross-linkable site was provided to compensate for the problem, and the adhesion

strength and mechanical properties were improved, and the long-term stability and performance of the electrode were studied.

1-4. PVDF binder

PVDF has been widely used as an organic solvent soluble binder in LIBs with Si anodes mainly due to its appropriate adhesive strength with electrode materials, high electrochemical stability, wide electrochemical window, as well as its reasonable wettability toward polar electrolyte for facile diffusion of Li-ions to active material surface.¹⁴ PVDF is a semi-crystalline linear homopolymer.¹⁵ C-C and C-F bonds have strong bond strength. It is attached to Si particles only Van der Waals force between fluorine and hydrogen atoms.⁶ But PVDF does not provide satisfactory performance when implemented with very high capacity.

Several reasons exist, including: 1) It can react with metallic Li to form more stable Li_xF_y at high temperatures. Since the reaction between metal Li and PVDF is exothermic, it causes self-heating and thermal

runaway reactions.¹⁶ As a result, the adhesion of the electrode particles is peeled off and the capacity is continuously reduced. 2) PVDF easily swells or dissolves in organic solution. The adhesion with the electrode is easily lost at high temperature.¹⁷ 3) It is easy to aggregation due to its high viscosity. Aggregated particles block the conduction channels and reduce the rate of charge transfer.¹⁸ 4) As it is semi-crystalline with low elongation, there is no volume change to accommodate the volume change of the Si-based anode.¹⁹

1-5. PVDF Modification

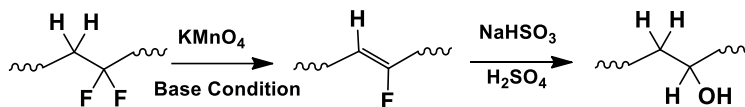
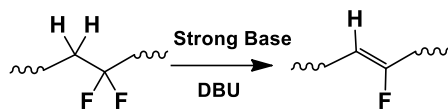
Polyvinylidene fluoride (PVDF) is widely adopted as a binder for lithium ion, lithium sulfur, lithium air and sodium batteries. The main advantages of PVDF as a binder are adhesive strength, high thermal stability, and wide electrochemical window. However, some intrinsic properties of PVDF, such as swelling and dissolution of organic electrolytes and low mechanical ductility, in the case of anodes in batteries, lead to crushing of the electrode long cycles.

Few strategies have been developed to improve the properties of Si-based anodes as binders. 1) Heat treatment. Improved lithium storage performance was obtained through heat treatment by Xu et al.²⁰ They found that the volume expansion of the Si electrode was significantly suppressed during the lithium insertion/extraction process depending on the annealing temperature. . 2) copolymerization. Wang et al. A robust block copolymer PVDF-b-Teflon (PTFE) binder for Si anodes was prepared.²¹ PVDF-b-PTFE binder exhibits large elongation at break of 250%, high viscosity, and high ionic conductivity, enabling long cycling stability of Si anodes. Efforts to modify the PVDF itself are not well considered. Since the chain is in an inactive state, a very harsh environment is required for modification. However, PVDF modification is possible even under mild conditions. First, the ATRP method via a metal catalyst can add desired functional groups to PVDF or PVDF-CTFE through this method. Another method is dehydrofluorination using a nucleophilic reaction for PVDF-HFP. This allows for much simpler methods and safer conditions than before. Finally, the method to be used this time is a method using dehydrochlorination of PVDF-

CTFE, a reaction that can be controlled with relatively weak base proceeds, and a double bond is formed after the reaction(Figure 4).



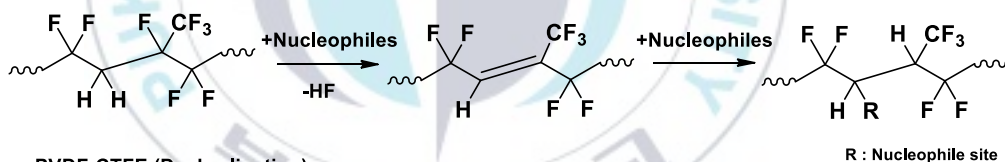
PVDF (Dehydrofluorination)



ATPR grafting



PVDF-HFP Modification (+Nucleophiles)



PVDF-CTFE (Dechlorination)

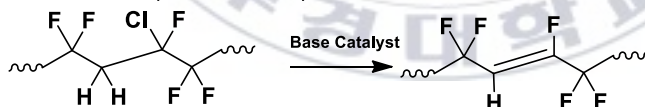


Figure 4. Modification methods of PVDF-based polymers

2. Experimental

2-1 Efficient binders for silicon-based lithium-ion battery

The reagents of the triethylamine (TEA, $\geq 99\%$), N-methylpyrrolidinone (NMP, $\geq 99\%$), tetrahydrofuran (THF, $\geq 99\%$), acetone ($\geq 95\%$), N,N-dimethylformamide (DMF, $\geq 99\%$), and methanol ($\geq 95\%$) were purchased from Sigma Aldrich. Poly(vinylidene fluoride) (PVDF) was purchased from Solvay Solexis (Solef 1015, 540 kg mol^{-1}). Poly(vinylidene fluoride)-(chlorotrifluoroethylene) (PVDF-CTFE) was received from Solvay Solexis (Solef 32008/1001, M_w : 480 kg mol^{-1} , 20.5 mol% of CTFE)

2-2. Synthesis of double bond-contained PVDF-CTFE (PVTD)

PVDF-CTFE (10 g, 20 mmol of Cl atoms) was added into a round-bottomed flask with 100 mL of NMP and stirred. Triethylamine (TEA, 13.8 mL (100 mmol)) was added into the above solution, and then the reaction was maintained for 96 h. The resultant was precipitated in excessive DI water. The precipitates were decanted and dissolved in THF. They were precipitated by pouring the solution in methanol with 1 vol% hydrochloric acid (HCl). The precipitation process was repeated 3-cycles, yielding PVTD ($M_{w,GPC}$: 616 kg mol^{-1} , M_w/M_n : 2.29). ^1H NMR (acetone- d_6 , ppm) : 6.0-6.7 (m, H-C=C-F) and 2.7-3.5(m, PVDF backbone). ^{19}F NMR (acetone- d_6 , ppm) : -89.3 ($-\text{CF}=\text{CHCF}_2\text{CH}_2\text{CF}_2-$), -92.7 ($-\text{CF}_2\text{CH}_2\text{CF}_2\text{CH}_2\text{CF}_2-$), -95.5 ($-\text{CFCICH}_2\text{CF}_2\text{CH}_2\text{CF}_2-$), -109.1 ($-\text{CF}_2\text{CH}_2\text{CF}_2\text{CF}_2\text{CFCl}-$) -109.3 to -110.8 ($-\text{CF}_2\text{CFCICF}_2\text{CFCICH}_2-$), -113.4 ($-\text{CF}_2\text{CF}_2\text{CF}=\text{CHCF}_2-$), -113.8 ($-\text{CF}_2\text{CH}_2\text{CF}_2\text{CF}_2\text{CF}=\text{CH}-$), -114.7 ($-\text{CF}_2\text{CH}_2\text{CF}_2\text{CF}_2\text{CH}_2-$), -117.0 ($-\text{CH}_2\text{CF}_2\text{CF}_2\text{CH}_2\text{CH}_2-$), -118.2 to -120.4 ($-\text{CH}_2\text{CF}_2\text{CF}_2\text{CFCICH}_2-$), -120.4 ($-\text{CH}_2\text{CF}_2\text{CF}_2\text{CF}=\text{CH}-$), and -120.4 to -123.3 ($-\text{CF}_2\text{CF}_2\text{CFCICH}_2\text{CF}_2-$).



2-3. Prepare of Electrode

Electrodes were prepared via typical slurry coating technique.

Polymer binders were dissolved in corresponding solvent (*N*-methyl-2-pyrrolidone (NMP)) and stirred for 12 h. Si 50 nm powders (12 Φ, surface area of 1.13 cm²

) and Super P (Shanghai Haohua Chemical Co., Ltd.) were added into above solutions (the mass ratio of Si powders, binder and [super](#) P was 6:2:2). The obtained slurry was coated on copper foil (Luoyang Hengsheng copper processing Co., Ltd.), dried at 150 °C under vacuum for 24 hr, and cut into 14 mm diameter disks. The calculated mass loading of silicon is about 0.6–0.7 mg cm⁻² on the electrode.

2-4 Characterization

^1H and ^{19}F NMR spectra were performed using a JNM ECZ-400 400 MHz spectrometer (JEOL Ltd. Japan) with acetone- d_6 solvent. The Fourier transform infrared (FT-IR) measurement was performed by a spectrometer (Nicolet iS10, USA). The thermal stability was evaluated by TGA (N-1000, Scinco, Korea) at N_2 atmosphere. The thermal properties were analyzed using differential scanning calorimetry (DSC, DSC-2910, Perkin Elmer, USA) at N_2 atmosphere from -80 to $200\text{ }^\circ\text{C}$ with $10\text{ }^\circ\text{C min}^{-1}$ scan rate. The mechanical properties of the film-type specimens were tested by a universal testing machine (UTM, AGS-10kNX Shimadzu, Japan) according to ASTM D638. For UTM tests, the solution-casted film specimens' width, length, and thickness were 10 mm, 4 mm, and 0.2 mm, respectively. The electrolyte contact angle test was performed using Phoenix-150 Touch (SEO, Korea). The rheological properties were measured by rheometer (MCR 302e, Anton Paar, Austria). Molecular weight was measured by a SHIMADZU, Nexera GPC system equipped with a differential RID-20A detector in DMF as

the mobile phase at 40 °C with a flow rate of 1 mL/min. The samples were separated through two columns: Shodex-GPC KD-804 and KD-805. Optical microscope for film samples was measured using I-CAMSCOPE.



2-5. Electrochemical characterization

The electrochemical property of prepared electrodes were measured in 2032-type coin cell, using Li foil as the counter electrode, Celgard 2400 polyethylene membrane as the separator, 1 M LiPF₆ in ethylene carbonate (EC) and diethylene carbonate (DEC)(1:1, v/v) with 10 wt% fluoroethylene carbonate (FEC) as the electrolyte, assembled in an Ar-filled glove box. Galvanostatic charge/discharge test was performed over a voltage range of 0.01–2 V at room temperature by a battery tester (CT2001A, LAND Battery Program-control Test System, China). An electrochemical workstation (CHI 660B) was used to carry out [cyclic voltammetry](#) (CV) in the voltage range of 0.01–5 V (vs Li/Li⁺)

3. Result and Disscusion

3.1 Strategy of Cross-linked PVDF-Based Polymers (PVTDX)

The expansion of the polymer binder causes a fracturing and fragmentation, followed by the decrease of electro capacity and poor cycling stability. Generally, the liner polymer binders such as PVDF and PVDF-CTFE have a critical disadvantage in electrochemical performance due to the lack of effective repairing properties of electrode damage caused by the expansion/shrink cycles (Fig. 5a). In this regard, to improve the electrochemical performance of Si anode, the cross-linked polymer binder (PVTDX) was conceptually designed, which improve not only the dimensional stability against volume change during operation but also the mechanical properties of the binder (Fig. 5b). These crosslinking structure of PVTDX was achieved by simple thermal crosslinking reaction of double bond in PVTD structure. The

rubber properties of the PVTDX binder due to the cross-linked structure were expected to have a positive effect on the Si anode.

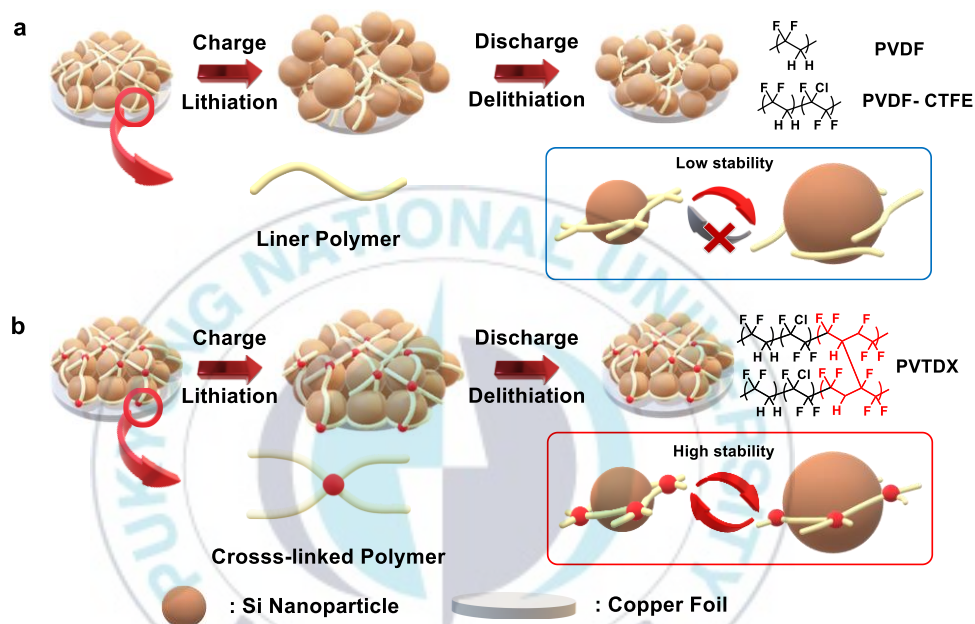


Figure 5. Schematic mechanisms for Si anode with (a) conventional leaner PVDF binders (PVDF and PVDF-CTFE) and (b) cross-linked PVDF binder (PVTDX).

3-2 Strategy of Cross-linked PVDF-Based Polymers (PVTDX)

The PVTD was synthesized from PVDF-CTFE by dehydrochlorination reaction with simple addition of TEA (Fig. 6). The double bonds (vinyl group) in PVTD main chains are important point of forming a crosslinking structure through heat treatment. The chemical structure of the synthesized PVDF-CTFE and PVTD were analyzed by ^1H NMR as shown in Fig. 7a. The characteristic peak of the PVDF was confirmed both PVDF-CTFE (black line) and PVTD (red line) at 2.7-3.5 ppm. The newly generated peak at 6.0-7.0 ppm in PVTD correspond to the protons on the vinyl group ($-\text{CF}_2-\text{CF}=\text{CH}-\text{CF}_2-$) derived from the dehydrochlorination reaction of PVDF-CTFE.^{22,24} Therefore, the main chain composition of the Resultant copolymers, including Double bonds could be calculated by eqn (1)

$$\text{Double bond} = \frac{2I_2}{I_1 + 2I_2} \times 100 \text{ mol\%} \quad \dots\dots(1)$$

In this formula, I_1 and I_2 are integral values of the NMR peaks at 2.7 to 3.5 ppm and 6.0 to 7.0 ppm, respectively.

The characteristic peak of generated vinyl structure of PVTD was also observed by ^{19}F NMR spectra (Fig. 7b). The peaks were appeared around -94.0, -109.1, -120.3, and -121.5 ppm corresponding to the tail-to-tail structure of VDF-CTFE. The head-to-tail structure (-CH₂-CF₂-CH₂-CF₂-) of VDF-VDF sequence was also observed at -92.7 ppm.^{22, 24} After the dehydrochlorination reaction (PVTD), new peaks were detected at -89.3, -113.4, and -113.8 ppm, which could be a vinyl group of PVTD structure. Furthermore, the characteristic peak of vinyl group (-C=C- stretching) was observed at around 1700 cm⁻¹ from FT-IR spectra (Fig.8).

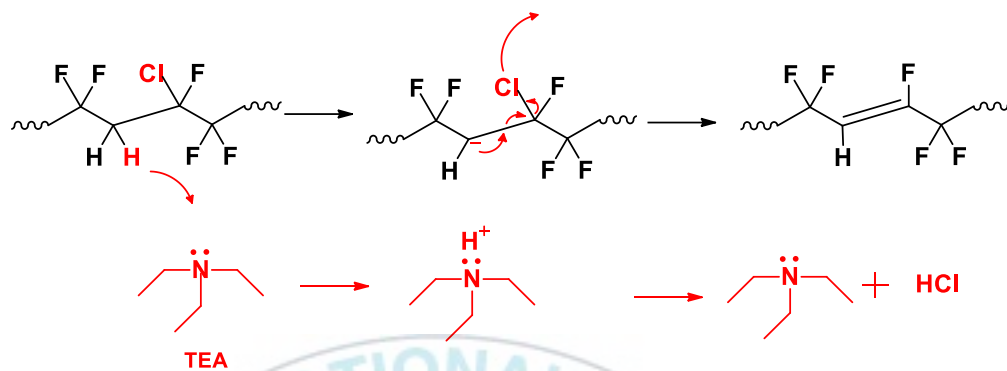


Figure 6. Mechanism of PVTD Synthesis (Using Dehydrochlorination of PVDF-CTFE).

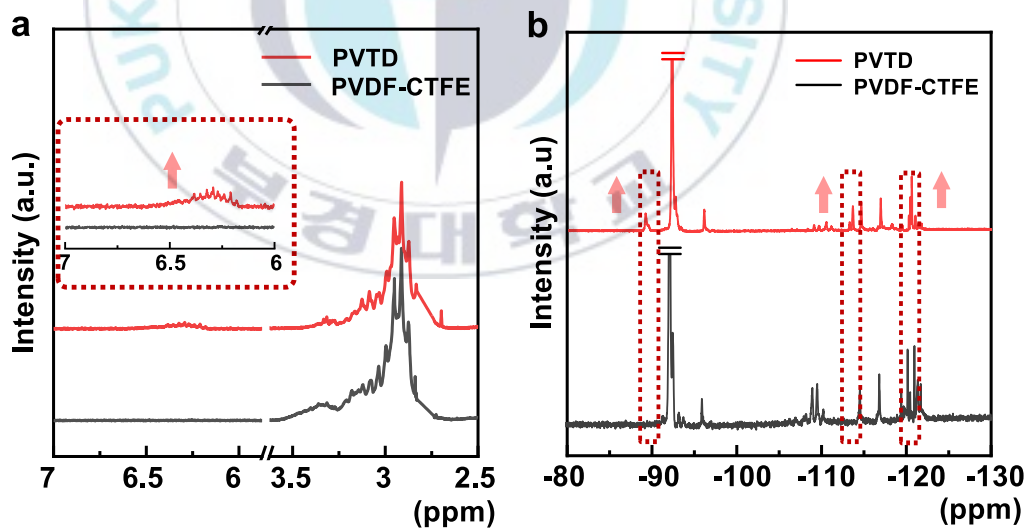


Figure 7. (a) ^1H NMR and (b) ^{19}F NMR of PVDF-CTFE and PVTD.

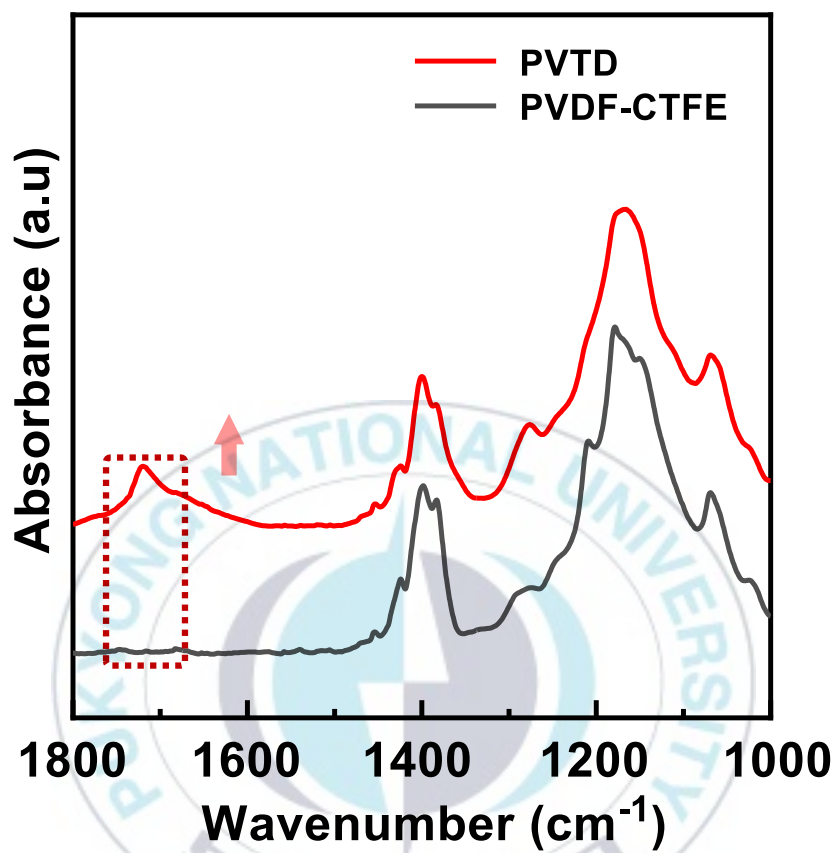


Figure 8. FT-IR spectra of PVDF-CTFE and PVTD.

3-3 Processibility of PVTDX Binder

PVDF is likely to accumulate due to its high viscosity, blocking conducting channel and decrease charge-transfer rate. This reaction through the dehydrochlorination reaction of PVDF-CTFE is accompanied by a change in chemical structure. PVDF is basically an α -based trans structure whereas PVTD has cis-trans isomerization due to the introduction of vinyl groups.²⁵ (Fig. 9a). These changes of chemical structure affect the rheological properties of the samples, which analyzed by complex viscosity with frequency sweep (Fig. 10). The complex viscosity of the PVTD was decreased in all frequency ranges than PVDF and PVDF-CTFE, which indicated that the introduction of the vinyl group changes the viscosity of the polymer solution due to the high chain mobility derived from cis-trans isomerization.²⁶

Furthermore, the loss tangent values of the PVTD was increased rather than PVDF and PVDF-CTFE due to the in presence of Cl atoms and vinyl group in the PVDF chain, which shows more viscous property. It was expected that the enhancement of the viscous properties

of PVTd could be improve the processability of the electrode. The configuration changes by the presence of double bonds were confirmed by FT-IR (Fig. 9b) . The PVTd spectrum showed the α -phase (trans) reduction with a increase of β -phase (cis) compared to those of PVDF-CTFE and PVDF, indicating an increase of randomness in the constituent structure.²⁷ The significantly lower viscosity and solution properties can be attributed to cis-trans isomerization due to the presence of 20 mol% double bonds in the PVTd backbone, which can significantly reduce the degree of crystallinity (ΔH_{PVTd} : 11.4 J g⁻¹ vs ΔH_{PVDF} : 33.1 J g⁻¹ versus $\Delta H_{\text{PVDF-CTFE}}$: 15.1 J g⁻¹) due to the mixed configuration (Fig. 11).

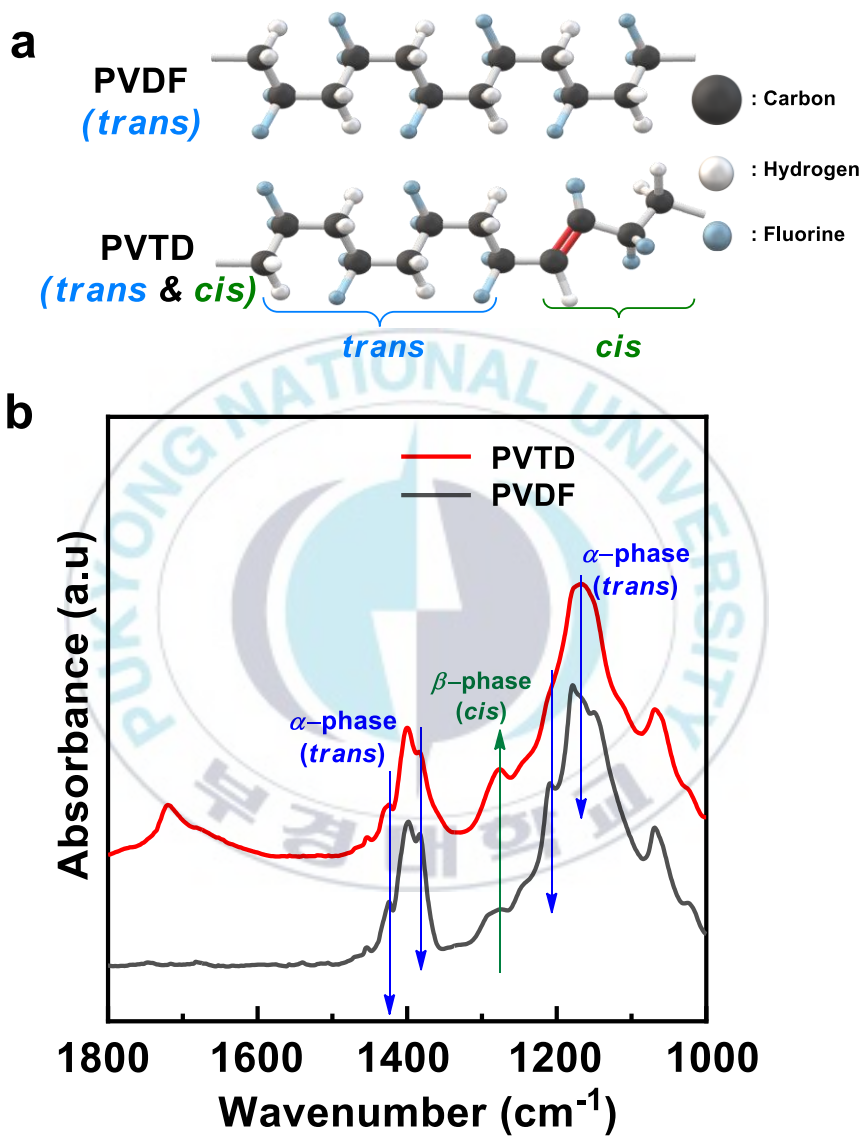


Figure 9. (a) Chemical structure of PVDF and PVTD with their crystalline phases. (b) FT-IR Spectra

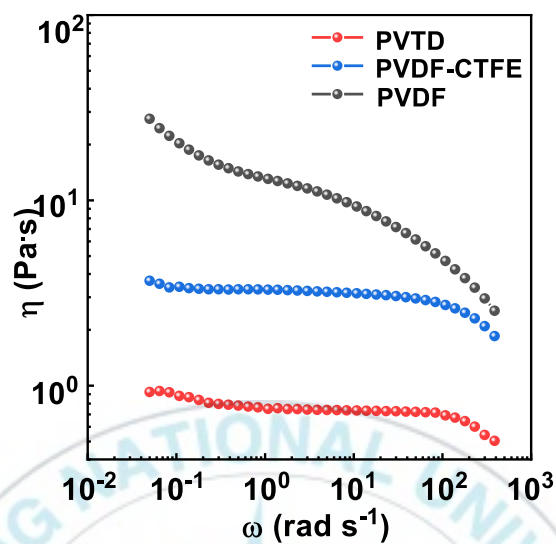


Figure 10. Complex viscosity curves of PVDF,PVDF-CTFE and PVTD

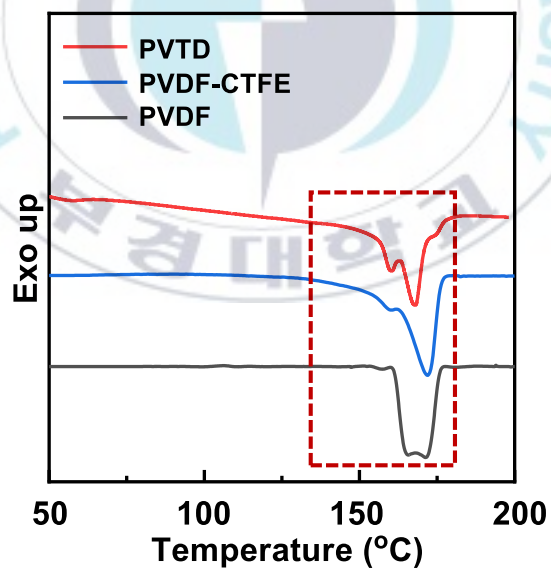


Figure 11. DSC data of PVDF,PVDF-CTFE and PVTD

3-4. Cross-link of PVTDX Polymer Binder

The Vinyl group (20 mol%) in PVTD are partially distributed on the PVDF backbone. It was expected that the PVTD could strategically induce the intra- and interchain cross-linking (PVTDX) by thermal post-treatment after the electrode fabrication. The cross-linking process on the electrodes may facilitate enhanced mechanical strength, thermal stability, chemical resistance, and recovery properties from the external force compared to PVTD and better than conventional PVDF-based binders.^{28,29,30,31} The PVTD chains could be covalently cross-linked to each other by self-crosslinking reaction by generated radicals derived from double bond in PVTD main chains. Those were motivated to clarify the cross-linking conditions. From the DSC heating curves, this research confirmed the melting temperature (T_m) of PVTD and PVTDX at around 150 °C (Fig. 13). Particularly, the exothermic peak of curing temperature (T_{cure}) was observed at 114 °C.³² In addition, the broad melting peak for PVTD was observed, ranging from 135 °C to 185 °C. Based on curing and melting peaks, this research strategically set up the

optimal curing conditions at 150 °C for 24 h (Fig. 12). The curing time was considered to remove heavy solvents (i.e., NMP for the electrode slurry). After the cross-linking treatment, yielding PVTDX, its plausible chemical structure is illustrated in Fig .12.

The cross-linked structure of PVTDX was also identified by the FT-IR spectra as shown in Fig. 14. The intensity of characteristic peak around 1700 cm^{-1} corresponding to double bond ($-\text{C}=\text{C}-$) of PVTDX was significantly reduced by self-crosslinking reaction of the double bond in PVTD chains.²⁹

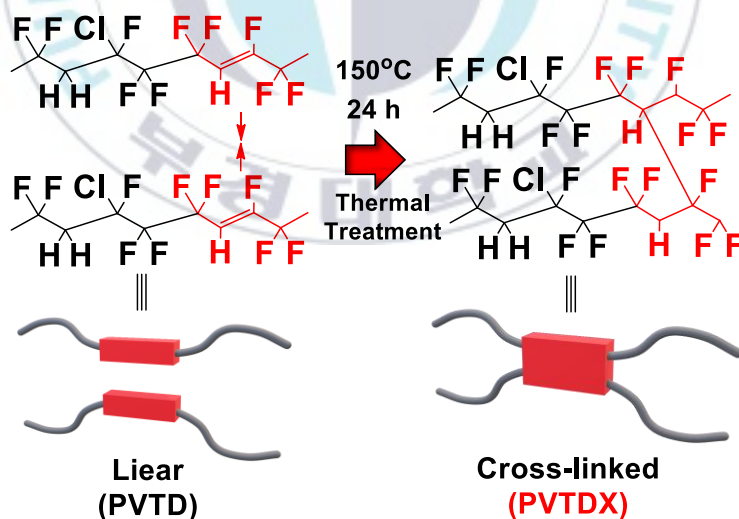


Figure 12. The schematic illustration for before and after a cross-linking process of PVTD

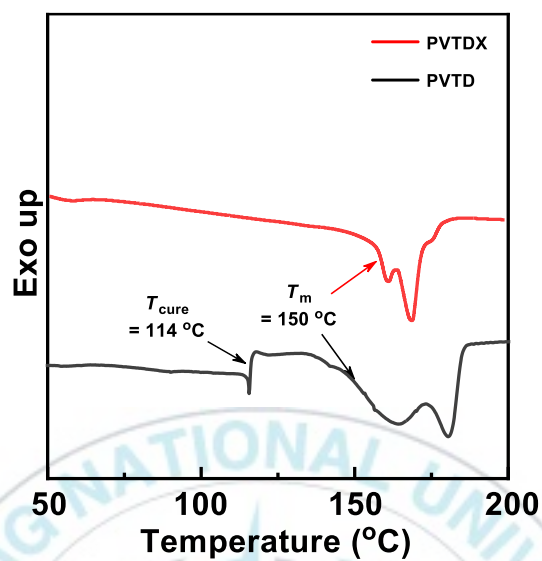


Figure. 13. 1st run DSC heating curves for PVTD and PVTDX.

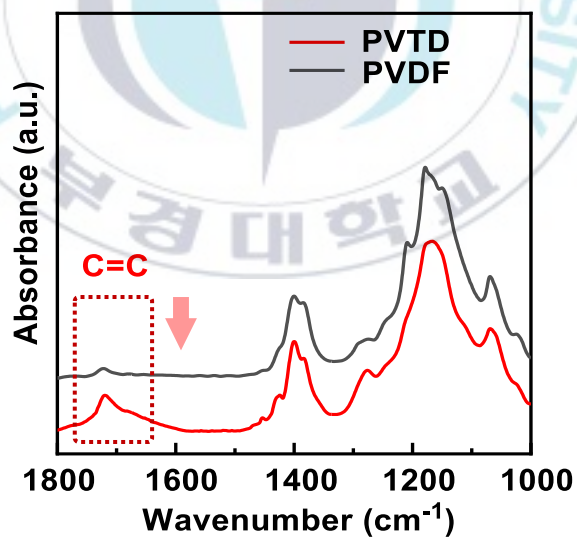


Figure. 14. FT-IR spectra for PVTD and PVTDX.

The solvent resistance test for PVTD and PVTDX films was performed using a good solvent (i.e., DMF) for the PVTD, resulting in that the PVTDX film showed better solvent resistance, while the PVTD film was entirely degraded (Fig. 15a). PVTDX showed the slight brownish color change of the solvent after 24 hr. It can be attributed to some of the PVTD chains being dissolved in DMF, and it may be explained by the partially cross-linked polymers containing the DMF soluble PVTDX polymers with low cross-linking density. The GPC characterization for the PVTD and PVTDX leached-out solution well supported our suggestion. PVTD GPC curve showed only one peak at M_w 616 kg mol⁻¹, However, the PVTDX GPC curve showed multi-modal peaks including small molecular weight M_w : 210 kg mol⁻¹ and large molecular weight M_w : 1,140 kg mol⁻¹ with 50% vs 50% area compositions (Fig. 15b). In addition, the insoluble PVTDX film in Fig. 8a can be relatively super-high molecular weight derived from interchain cross-linking. Accordingly, low molecular weight and high molecular weight polymers are mixed in PVTDX.

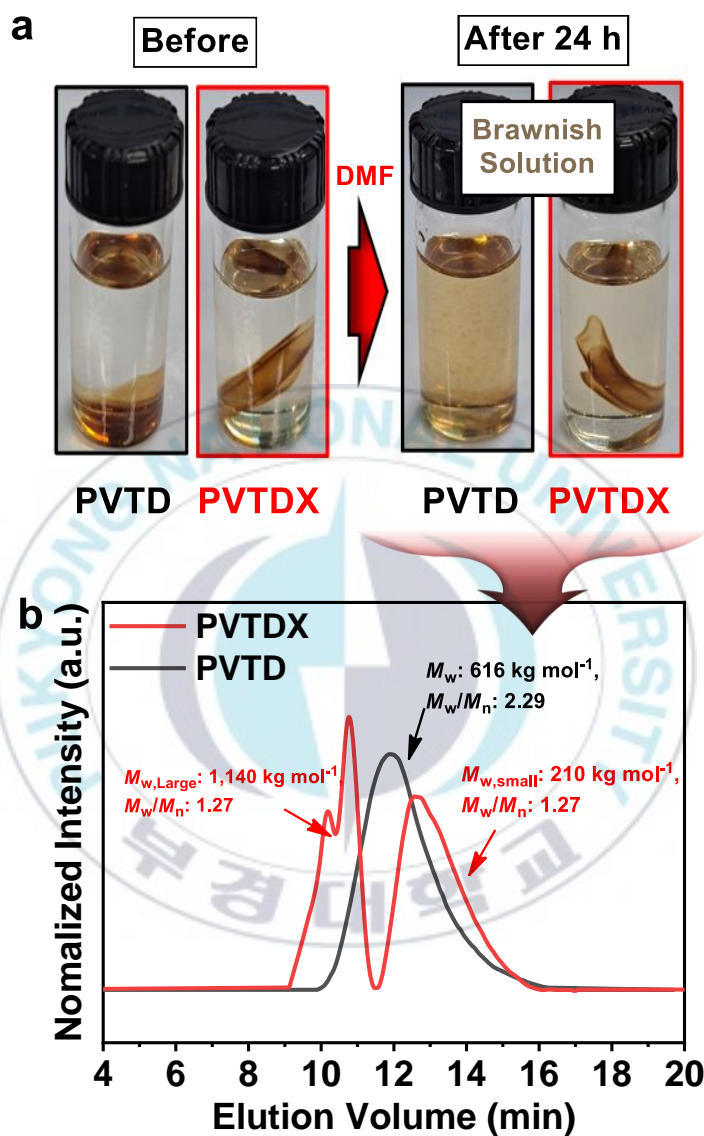


Figure 15. (a) Photographs for the solvent resistance test in DMF before and after 24 h later. (b) GPC Data of DMF solution at 24hr after.

Tensile tests were performed for PVTD and PVTDX, resulting in that the PVTDX showed the highest tensile strain and strength compared to the PVTD (Fig. 16). Notably, the PVTDX exhibited an increase in tensile strength and strain relative to those of PVTD. The increase of the tensile strength for PVTDX can be ascribed to the cross-linking effect. However, the strain increase cannot explain only for cross-linking effect. It can be explained also partially cross-linked state of PVTDX. Ma et al. reported a partially cross-linked poly (butylene succinate) (PBS) using dicumyl peroxide (DCP) radical initiator.³² The cross-linked PBS (PBSX) exhibited 1.6-fold increased strain relative to that of the PBS. In addition, PBSX also exhibited clear T_m peaks with a decrease in the heat of fusion (ΔH_m) which is correlated to a reduction of crystallinity. In this regard, the heat of fusion (ΔH_m) also calculated by the PVTD and PVTDX, yielding 11.4 J g^{-1} to 7.7 J g^{-1} , which are in good agreement with Ma's report as mentioned above.³² The TGA test for PVTDX was performed to define the more stability compared to PVTD. The initial decomposition temperature (T_{dec}) at 95% residue of the PVTDX was noticeably increased than PVTD because of more

covalent bond between chains in PVTDX such as crosslinking structure, sequentially followed by PVTDX (425 °C) > PVTD (368 °C) (Fig. 17). It means that the crosslinking of the PVTDX can increase the thermal stability of the copolymer binder than PVDX.

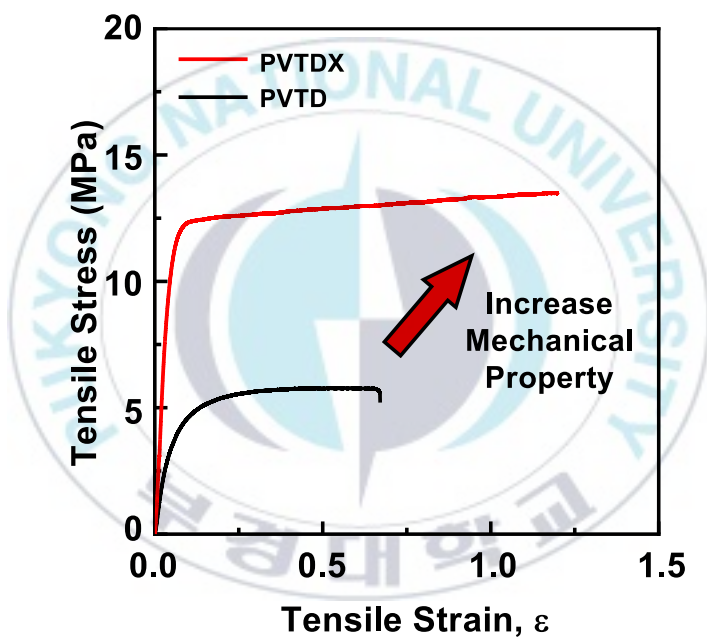


Figure. 16. S-S curves of PVTD, and PVTDX

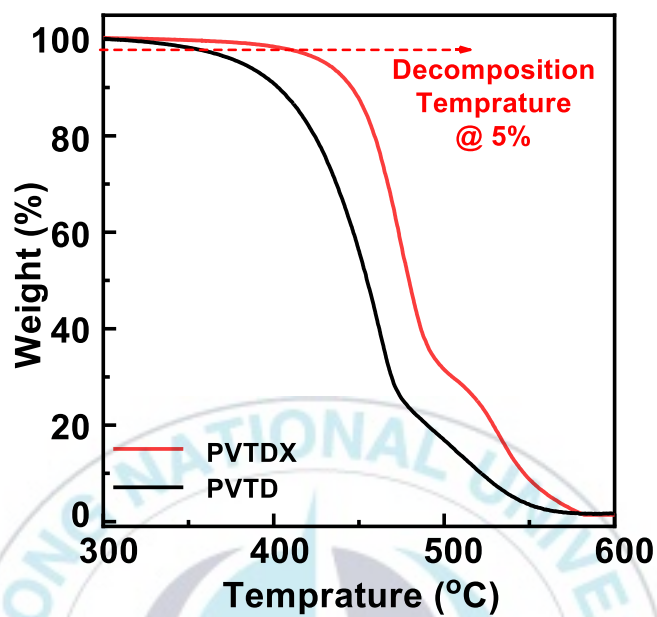


Figure 17. TGA (inset: 5% degradation point) of PVTD and PVTDX

3-5. Electrochemical Performance of PVTDX Binder

Figure 18 a and b show the cyclic voltammogram (CV) of Si anode of PVDF and PVTDX at 1A g⁻¹. the following anodic and cathodic scans, the Lithiation(cathodic) peaks at ~0.19 V and anodic peaks at 0.36 V and 0.51 V are observed, which are attributed to the behavior of amorphous Si and Li alloy/dealloying.³³

Meanwhile, the alloying peak at ~0.20 V and the dealloying peaks at ~0.36 and 0.51 V gradually increase with charge/discharge cycles due to activation of the hierarchical micro-sized crystal Si, which has been reported in Si anode.^{34,35} Increase in lithiation/delithiation peaks compared to PVDF. PVDF-CTFE basically has higher ionic conductivity than PVDF.³⁶ For this reason, the progress of the with lithiation/delithiation process appears more clearly in the progress of the CV test.

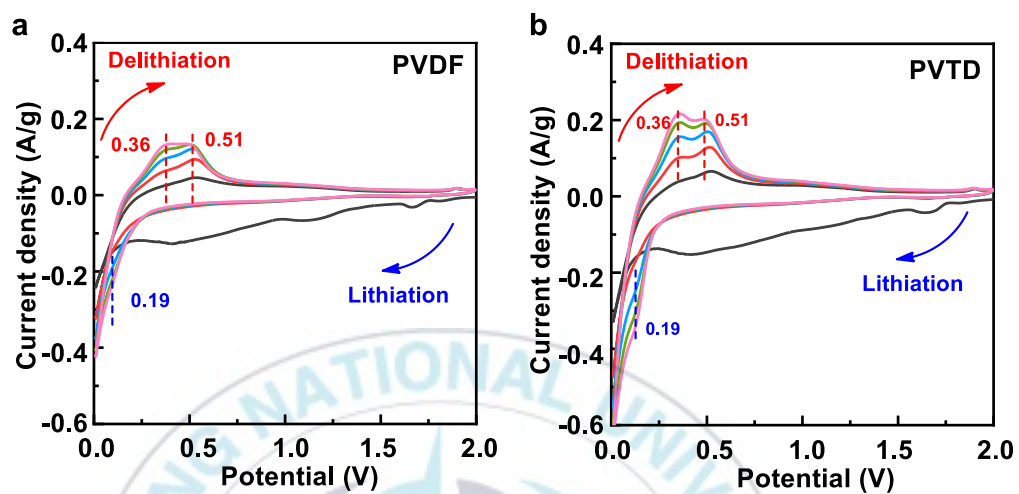


Figure 18. Cyclic voltammetry curves of silicon anode with (a) PVDF and (b) PVTDX binder.

Figure 19a and b shows the long cycle performance of the evaluated PVDF and PVTDX (Si anodes made with PVDF and PVTDX binders). Constant-current charge-discharge measurements for the potential range of 0.01-1.2 V at 1 A g^{-1} show a long plateau in the discharge curve at $0.2 \sim 0.01 \text{ V}$, which is consistent with what appears in the Li/Si alloy curve. PVTDX had very poor cycling performance with 10^{th} delithiation capacity reaching 1729 mAh g^{-1} and 100^{th} to 936 mAh g^{-1} , while PVDF had very poor cycling performance with 10^{th} to 1276 mAh g^{-1} and 100^{th} to 256 mAh g^{-1} .

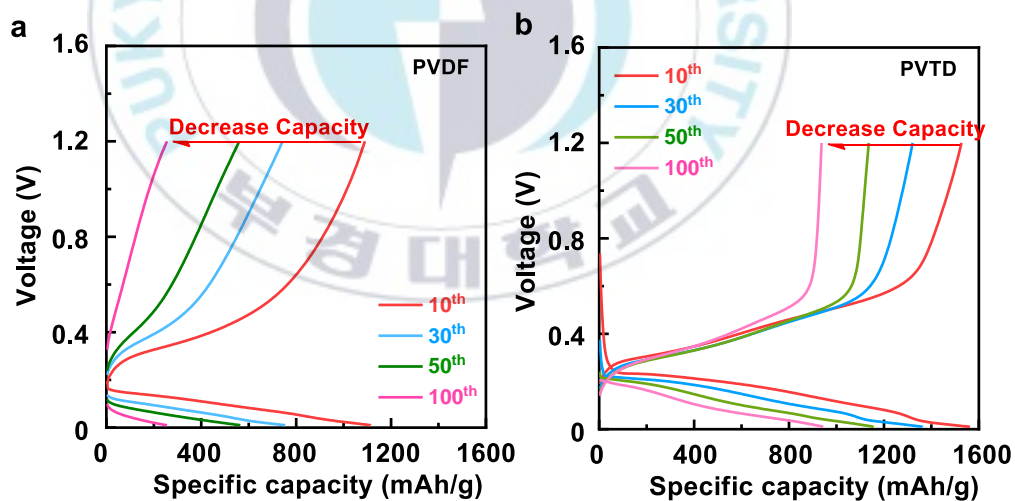


Figure. 19. Charge/discharge profiles at 10^{th} , 30^{th} , 50^{th} and 100^{th} of silicon anode with (a)PVDF and (b)PVTDX binder.

Figures 20 a and b shown the rate performance of PVDF, PVDF-CTFE and PVTDX. PVTDX electrodes can recover to the original capacity value after different current charge/discharge process, and the higher specific capability. At a large current density of 5 C, the PVTDX exhibits a high capacity, about 400 mAh g⁻¹. By contrast, PVDF and PVDF-CTFE delivers a low capacity of under 50 mAh g⁻¹ and cannot recover to original capacity (Fig. 20a). In Figure 10d, each electrode was measured for 100 charge/discharge processes within a constant (1 A g⁻¹) current. In continuous cycling, PVTDX showed a capacity decrease of about 1737 mAh g⁻¹ to 957 mAh g⁻¹. However, in the case of PVDF, stability is greatly reduced from 1276 mAh g⁻¹ to 252 mAh g⁻¹ after 100 cycles. Through this, it was confirmed that the stability of the electrode was greatly improved.

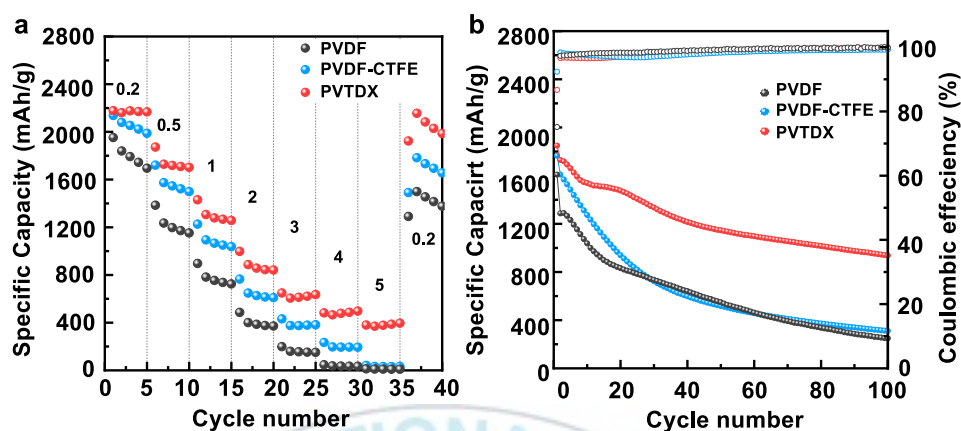


Figure. 20. (a) Rate capability at various current densities. (b) Cycling performance at 1 A/g.

High capacity at high current density leads to higher ionic conductivity and faster charge transfer, and the improved rate and recovery performance of PVTDX may be related to the excellent mechanical properties of the binder and the stable polymer properties in the electrolyte (Fig. 21). The tensile stress-strain curves of PVDF, PVDF-CTFE and PVTDX film were shown in Fig. 2e. This curves of the polymers demonstrate that cross-linking enhance the mechanical performance. PVDF show a high tensile strength (11.7 MPa) but low elongation (2.27 %), indication brittle performance . PVDF-CTFE

shown a better elongation (4.12 %) but lower strength (7.7 MPa) than PVDF. However, PVTDX show not only high strength (13.5 MPa) but also high elongation (ca. 120.0 %).

PVDF-based polymers have high affinity for electrolyte, which is advantageous for electrode ion conduction, but on the other hand, the electrode is swelled by the electrolyte and the electrode is peeled off from the current collector, and the electrode structure is easily degrade.³⁷ High stability can bring advantages for electrode retention, this research investigated electrolyte stability testing for PVTDX compared to conventional PVDF binders(Fig. 22).

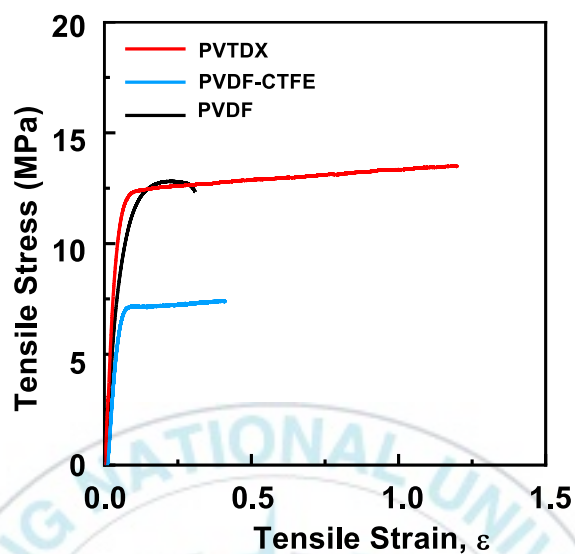


Figure. 21. S-S curves of PVDF, PVDF-CTFE and PVTDX,

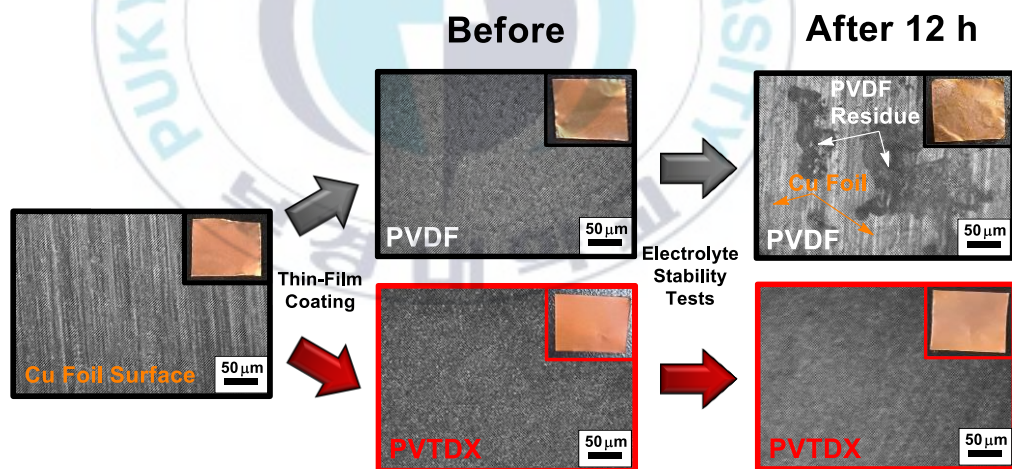


Figure. 22. Before and after electrolyte stability tests at RT (1 M LiPF₆ in EC/DEC (50:50 v/v): OM images of PVDF and PVTDX thin films (inset: their photographs).

3-6. SEI Contribution of PVTDX Binder

The formation of the unstable solid-electrolyte interphase (SEI) layer leads to improved capacity retention and better cycle life of the Si anode. The polymer binder participates in formation a stable SEI layer and affects several factors.²² However, this SEI layer also collapses or excessively expands during the expansion/contraction cycle of Si. Fig. 23a is a comparison of the SEI layer before and after 100 cycles according to the binder. PVDF, a linear polymer that lacks expansion inhibition, expanded nearly 4.8 times increase(17.25 μm to 82.48 μm) after cycling. In contrast, PVTDX was only 1.6 times increase(14.52 μm to 23.59 μm) through successful suppression.(Fig. 23a) Through this, it was confirmed that PVTDX helped to maintain a stable SEI layer.^{30,38}

In the case of an unstable solid-electrolyte interphase SEI layer, the electrolyte is separated due to continuous decomposition. The SEI layer formed by reductive decomposition of the electrolyte component causes irreversible capacity loss, which negatively affects the battery cable.

The Li_xPF_y layer is generated due to continuous decay and regeneration of the SEI layer, or a layer having an insulating property such as $\text{C}=\text{O}$ is generated due to oxidation.⁴⁰ The effect of the binder on this was measured by XPS. (Fig. 23b, c, d) Relatively few SEI layers with insulating properties are generated in PVDF, but a larger number of insulating layers are generated in PVDF.

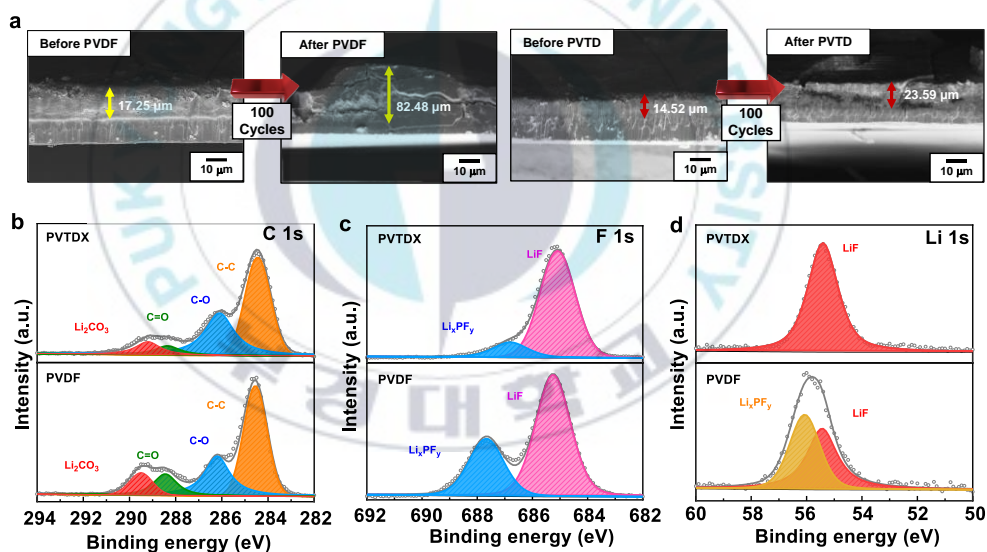


Figure. 23. Cross-section SEM images of silicon anode before and after cycling with (a) PVDF, and PVTDX binders. XPS spectra of (b) C 1s, (c) F 1s and (d) Li 1s peaks on the surface of silicon anode with PVDF and PVTDX binders after 100 cycles.

3-7. Interfacial Adhesion with Electrode

Low adhesion and cohesion between binders, active materials, and current collector will give rise to capacity decrease and poor cycle stability. A peel test was performed to compare the adhesion performance between PVDF and PVTDX at the interface (Fig. 24a). And the peel test was identified by the 90° detachmant on the surface. Peeling of the surface was confirmed by a 180° peel test (Fig. 24b, c). The test value of the average adhesive force of PVDF is $0.02\text{N}\cdot\text{mm}^{-1}$, and PVDF-CTFE shows an extreme force of 0.08N. And PVTD binder shows strong adhesion(0.48 N mm^{-1}).

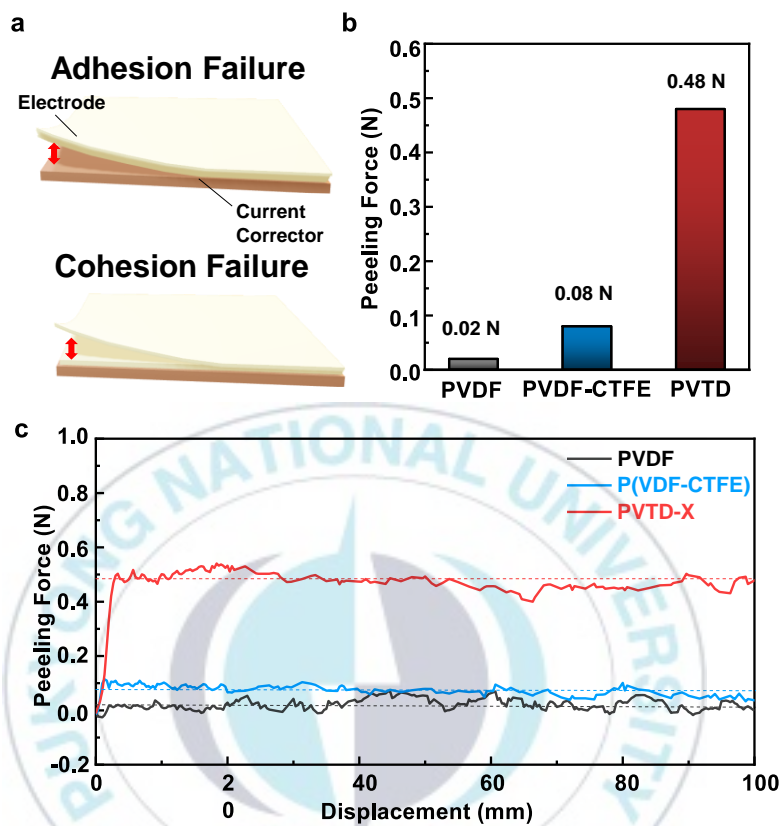


Figure 24. (a) Adhesion and Cohesion illustrate. Adhesive properties of the silicon anode using different binders : (b) Force-displacement curves and (h) peel strength.

4. Conclusion

Silica anode is valuable as a new LIB material with high efficiency, but there are limitations in its use as it has adverse effects such as volume expansion and rapid reduction in efficiency. In order to solve this problem, based on PVDF, which is the most used commercially among binder systems studied recently, this research tried to improve the performance by developing a cross-linked polymer rather than a linear polymer.

The synthesized PVTD was confirmed by ^1H NMR, ^{19}F NMR, and FT-IR. Polymer type in which a vinyl group was introduced was made based on PVDF-CTFE. After that, the crosslinking reaction was carried out by heating at 150°C , and it was confirmed that the crosslinking was partially done, and as a result, it was confirmed that the stress-strain increased at the same time.

For the preparation of the electrode, PVTD was dried at 150°C . for 24 hr at the same time as cross-linking. Compared with commercial PVDF, electrode efficiency, stability, retention of SEI layer, and

adhesion performance are all improved. Research on the improvement of PVDF by such crosslinking is expected to improve the performance of PVDF, which has been limited so far, and to utilize the Si anode as an electrode



Reference

- [1] A.N.Dey. (1971) Electrochemical Alloying of Lithium in Organic Electrolytes. *Journal of The Electrochemical Society*. 118. 1547–1549
- [2] D.Ma, Z.Cao & A.Hu. (2014) Si-Based Anode Materials for Li-Ion Batteries: A Mini Review. *Nano-Micro Letters*. 6. 347–358
- [3] H.K. Chae et al., (2003), A route to high surface area, porosity and inclusion of large molecules in crystals. *Nature*. 427.523-527
- [4] S.Uchida et al. (2015) Electrochemical properties of non-nano-silicon negative electrodes prepared with a polyimide binder. *Journal of Power Sources*. 273. 118-122
- [5] S.Chae.(2017) Confronting Issues of the Practical Implementation of Si Anode in High-Energy Lithium-Ion Batteries. *Joule*.1. 47-60
- [6] D. Mazouzi. et al.(2015) Critical roles of binders and formulation at multiscales of silicon-based composite electrodes. *Journal of Power Sources*. 280. 533-549
- [7] H,Chen et al.(2018) Exploring Chemical, Mechanical, and Electrical Functionalities of Binders for Advanced Energy-Storage Devices. *Chemical Reviews*. 118. 8936-8982

- [8] T. Kwon, J.W.Choi and A.Coskun.(2018) Prospect for Supramolecular Chemistry in High-Energy-Density Rechargeable Batteries. *Joule*. 3. 662–682
- [9] V. Wenzel, H. Nirschl and D. Ntzel.(2015) Challenges in Lithium-Ion-Battery Slurry Preparation and Potential of Modifying Electrode Structures by Different Mixing Processes. *Energy Technol.* 3. 692-698
- [10] S.L.Choun et al .(2014) Small things make a big difference: binder effects on the performance of Li and Na batteries. *Physical Chemistry Chemical Physics*. 16. 20347-20359
- [11] Y. Cho et al. (2019) A Pyrene–Poly(acrylic acid)–Polyrotaxane Supramolecular Binder Network for High-Performance Silicon Negative Electrodes. *Advanced Material*. 31. 1905048
- [12] Y.Yang. et al.(2021) Towards efficient binders for silicon based lithium-ion battery anodes. *Chemical Engineering Journal*. 406. 126807
- [13] J.S. bridel et al.(2010) Key Parameters Governing the Reversibility of Si/Carbon/CMC Electrodes for Li-Ion Batteries. *Chemistry of Materials*. 22. 1229-1241

- [14] H. Yuan. et al.(2018) A Review of Functional Binders in Lithium–Sulfur Batteries. *Advanced Energy Material.* 8. 1802107
- [15] H. Lefebvre, F.Bauer and L. Eyraud.(1995) Optimization and characterization of piezoelectric and electroacoustic properties of PVDF- β induced by high pressure and high temperature crystallization. *Ferroelectrics.* 171. 259-269
- [16] A. D. Pasquier et al.(1998) Differential Scanning Calorimetry Study of the Reactivity of Carbon Anodes in Plastic Li-Ion Batteries. *Journal of The Electrochemical Society.*145. 472
- [17] E.Tsuchida, H. Ohno and K. Etsunemi.(1983) Conduction of lithium ions in polyvinylidene fluoride and its derivatives—I. *Electrochimica Acta.* 28. 591-595
- [18] E J. Patra et al.(2019) Moderately concentrated electrolyte improves solid–electrolyte interphase and sodium storage performance of hard carbon. *Energy Storage Materials.* 16. 146-154
- [19] P.T. Dirlam, R.S. Glass, K.Char and J. Pyun (2017) The Use of Polymers in Li-S Batteries: A Review. *Journal of Polymer Science.* 55. 1735-1668

- [20] Y.H. Xu et al. Simple annealing process for performance improvement of silicon anode based on polyvinylidene fluoride binder. *Journal of Power Sources*. 195. 2069-2073
- [21] X. Wang et al.(2020) Highly Elastic Block Copolymer Binders for Silicon Anodes in Lithium-Ion Batteries. *ACS Applied materials & interfaces*. 12. 38132-38139
- [22] S. Tan, J. Li, G. Gao, H. Li and Z. Zhang.(2012) Synthesis of fluoropolymer containing tunable unsaturation by a controlled dehydrochlorination of P(VDF-co-CTFE) and its curing for high performance rubber applications. *Journal of Materials Chemistry*. 22. 18496
- [23] Z. Y. Yang, (2003) Addition reaction of halogens to vinyl (pentafluorocyclopropanes): Competition between a radical addition and an electrophilic addition. *Journal of Organic Chemistry*. 68. 5419-5421
- [24] Y. Lu, J. Claude, Q. Zhang, and Q. Wang.(2006) Microstructures and Dielectric Properties of the Ferroelectric Fluoropolymers Synthesized via Reductive Dechlorination of Poly(vinylidene fluoride-co-chlorotrifluoroethylene)s. *Macromolecules*. 39. 6962-6968.

- [25] Y. Ma, J. Ma and G. Cui.(2019) Small things make big deal: Powerful binders of lithium batteries and post-lithium batteries. *Energy Storage Materials*. 20. 146–175.
- [26] S. Janakiraman et al.(2019) Electrospun electroactive polyvinylidene fluoride-based fibrous polymer electrolyte for sodium ion batteries. *Materials Research Express*. 6. 086318
- [27] Z. Q. Wan et al.(2019) Reversible Transformation between Amorphous and Crystalline States of Unsaturated Polyesters by Cis–Trans Isomerization. *Angewandte Chemie International Edition*. 58. 17636-17640.
- [28] A. W. Martinez et al. (2014) Effects of crosslinking on the mechanical properties, drug release and cytocompatibility of protein polymers. *Acta Biomater*.10. 26-33
- [29] P. Parikh et al. (2019) Role of Polyacrylic Acid (PAA) Binder on the Solid Electrolyte Interphase in Silicon Anodes. *Chemistry of Materials*. 31. 2535-2544.

- [30] F. M. Uhl et al.(2001) The thermal stability of cross-linked polymers: methyl methacrylate with divinylbenzene and styrene with dimethacrylates. *Polymer Degradation and Stability*. 71. 317-325
- [31] F. Yang et al.(2020) Highly elastic, strong, and reprocessable cross-linked polyolefin elastomers enabled by boronic ester bonds. *Polymer Chemistry*. 11. 3285-3295.
- [32] J. P. Ma, Z. Ma, W. Dong, Y. Zhang and P. J. Lemstra. (2013) Structure/property relationships of partially crosslinked poly (butylene succinate). *Macromolecular Materials and Engineering*. 298, 910
- [33] F. m. Hassan et al.(2014) .Engineered Si Electrode Nanoarchitecture: A Scalable Postfabrication Treatment for the Production of Next-Generation Li-Ion Batteries. *Nano Letters*. 14. 277-283.
- [34] H. C. Tao, L. Z. Fans and X. Qu.(2012) Facile synthesis of ordered porous Si@C nanorods as anode materials for Li-ion batteries. *Electrochimica Acta*. 71. 194-200.
- [35] M. Ge et al.(2012) Porous Doped Silicon Nanowires for Lithium Ion Battery Anode with Long Cycle Life. *Nano Letters*. 12. 2318-2323.

- [36] R.E.Sousa et al.(2015) Poly(vinylidene fluoride-co-chlorotrifluoroethylene) (PVDF-CTFE) lithium-ion battery separator membranes prepared by phase inversion. *RSC Advanced*. 5. 90428-90436
- [37] K. L. Browning et al. (2020) The Study of the Binder Poly(acrylic acid) and Its Role in Concomitant Solid–Electrolyte Interphase Formation on Si Anodes. *ACS Applied Materials & Interfaces*. 12. 10018-10030.
- [38] J. M. Martinez de la Hoz, F.A. Soto and P.B. Balbuena et al. (2015) Effect of the Electrolyte Composition on SEI Reactions at Si Anodes of Li-Ion Batteries. *The Journal of Physical Chemistry C*. 13. 7060–7068.